Aligned Single-Wall Carbon Nanotube Polymer Composites Using an Electric Field

CHEOL PARK,[1] JOHN WILKINSON,[2] SUMANTH BANDA,[3] ZOUBEIDA OUNAIES,[3] KRISTOPHER E. WISE,[1] GODFREY SAUTI,[4] PETER T. LILLEHEI,[5] JOYCELYN S. HARRISON[5]

[1]National Institute of Aerospace, NASA Langley Research Center, Hampton, Virginia 23681

[2]Department of Electrical Engineering, Virginia Tech, Blacksburg, Virginia

[3]Department of Mechanical Engineering, Virginia Commonwealth University, Richmond, Virginia

[4]School of Physics, University of the Witwatersrand, Milner Park, Johannesburg, South Africa

[5]Advanced Materials and Processing Branch, NASA Langley Research Center, Hampton, Virginia 23681

Received 4 November 2005; revised 2 March 2006; accepted 24 March 2006
DOI: 10.1002/polb.20823
Published online in Wiley InterScience (www.interscience.wiley.com).

ABSTRACT: While high shear alignment has been shown to improve the mechanical properties of single-wall carbon nanotube (SWNT)-polymer composites, this method does not allow for control over the electrical and dielectric properties of the composite and often results in degradation of these properties. Here, we report a novel method to actively align SWNTs in a polymer matrix, which permits control over the degree of alignment of the SWNTs without the side effects of shear alignment. In this process, SWNTs were aligned via AC field-induced dipolar interactions among the nanotubes in a liquid matrix followed by immobilization by photopolymerization under continued application of the electric field. Alignment of SWNTs was controlled as a function of magnitude, frequency, and application time of the applied electric field. The degree of SWNT alignment was assessed using optical microscopy and polarized Raman spectroscopy, and the morphology of the aligned nanocomposites was investigated by high-resolution scanning electron microscopy. The structure of the field induced aligned SWNTs was intrinsically different from that of shear aligned SWNTs. In the present work, SWNTs are not only aligned along the field, but also migrate laterally to form thick, aligned SWNT percolative columns between the electrodes. The actively aligned SWNTs amplify the electrical and dielectric properties of the composite. All of these properties of the aligned nanocomposites exhibited anisotropic characteristics, which were controllable by tuning the applied field parameters. © 2006 Wiley Periodicals, Inc.* J Polym Sci Part B: Polym Phys 44: 1751–1762, 2006
Keywords: alignment; electric field; nanocomposite; photopolymerization; single-wall carbon nanotube

INTRODUCTION

Single-wall carbon nanotubes (SWNTs) have been considered for a number of applications because of their unique combinations of superb electrical, mechanical, and thermal properties.[1] Successful structural reinforcement of polymer matrices by SWNTs has been reported where significant improvement of mechanical properties was achieved at very low SWNT loadings.[2–7] Recently, sensing and actuating capabilities of SWNTs and SWNT-polymer composites have been studied in response to temperature,

Correspondence to: C. Park (E-mail: c.park@larc.nasa.gov)
Journal of Polymer Science: Part B: Polymer Physics, Vol. 44, 1751–1762 (2006)

chemical vapors, strain, stress, electrochemical, and electrical stimuli.[8–13] Shear forces have been frequently used for aligning inclusions along the flow direction to reinforce mechanical properties. Although shear alignment of SWNTs can improve mechanical properties in the shear direction, electric and dielectric properties tend to decrease along the shear direction as well as in the perpendicular direction with increasing SWNT orientation. Kumar et al.[6] showed that a well-aligned 10 wt % SWNT-PBO (poly(*p*-phenylene benzbisoxazole)) composite fiber exhibited an electrically insulating behavior while achieving significant mechanical reinforcement along the fiber direction. This loading level is at least two orders of magnitude higher than the percolation concentration of an unaligned SWNT polymer composite. This low conductivity can be understood by considering the low statistical probability of contacts among the aligned fibers along the orientation direction, which is consistent with the predictions of excluded volume theory.[14,15] These results indicate that shear alignment of SWNTs may not be a practical method of augmenting nanocomposite properties beyond mechanical reinforcement. The only way of circumventing this difficulty with shear processing would be to further increase the loading of SWNTs, which would limit its versatility for developing multifunctional materials for specific demands.

In the present report, a novel method is introduced which allows for control over the electrical and dielectric properties of a SWNT-polymer composite by aligning SWNTs under an AC electric field. Alignment of SWNTs by electric or magnetic fields has previously been reported,[16–20] though usually in dilute solutions during solvent evaporation or filtration. More recently, very limited alignment of SWNTs in a polymer matrix was achieved using a magnetic field[21] and a thermally cured aligned SWNT epoxy composite prepared under an electric field was reported.[22] In the present work, control over the degree of alignment of SWNTs in a photopolymerizable monomer solution was achieved by adjusting the applied field strength, frequency, and application time. The conductivity and dielectric properties can be tailored over several orders of magnitude by adjusting these parameters.

EXPERIMENTAL

The photopolymerizable monomer used in this study is a blend of urethane dimethacrylate (UDMA)

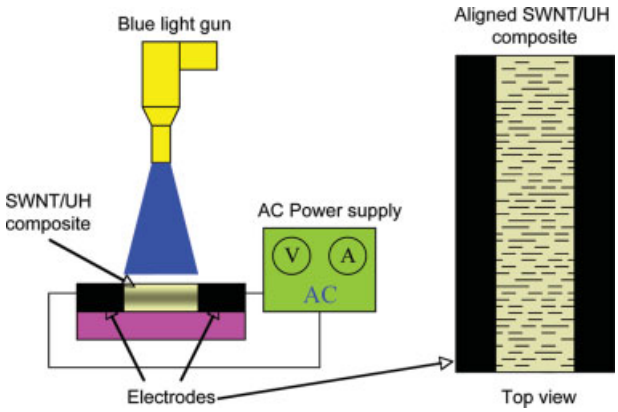

Figure 1. (a) Experimental setup of photopolymerization of SWNT/UH composite under an electric field; (b) top-view of the alignment cell (aligned SWNTs shown as discontinuous lines). [Color figure can be viewed in the online issue, which is available at www.interscience.wiley.com.]

and 1,6-hexanediol dimethacrylate (HDDMA) at the ratio of 9 to 1 (UDMA/HDDMA(9/1) = UH). The viscosities were 12.5 Pa·s and 7.0×10^{-3} Pa·s for UDMA and HDDMA, respectively.[23] Both UDMA and HDDMA monomers can be polymerized by blue light with camphorquinone as a photoinitiator and *N*,*N*-dimethylaminoethyl methacrylate as an accelerator. The monomers could be solidified to a depth of 3 mm within about 3 s under illumination by intense blue light. Single-wall carbon nanotubes (SWNTs) synthesized by a high-pressure CO (HiPco) method (CNI, TX) were used as multifunctional inclusions. A known quantity of SWNTs (fluffy powders) were added to the less viscous HDDMA monomer in a beaker and mixed vigorously by homogenizing for 10 min (750 rpm with a 6 mm diameter rotor homogenizer) and sonicated for an hour at 47 kHz. Then, the SWNT/HDDMA solution was mixed with the UDMA monomer with a mechanical stirrer to produce a 0.03% SWNT/UDMA/HDDMA(9/1) (= SWNT/UH) solution. The photoinitiator and accelerator were added into the SWNT/UH solution in a dark room. This solution was transferred into a microcuvet cell with electrodes on two narrow sides. A schematic of the alignment and photopolymerization apparatus is shown in Figure 1. Either a pure UH monomer solution or 0.03 wt % SWNT/UH composite solution was added in the 1 mm deep cell between the electrodes spaced at 2.3 mm. The 0.03 wt % concentration was selected as it is expected to be below the percolation threshold, based on previous percolation studies

of various SWNT-polymer composites.[24,25] This concentration also allows one to efficiently cure the control sample across its 1 mm thickness. An AC power supply (Trek model 50/750) and a function generator (Hewlett-Packard 33120A) were used to control the applied electric field conditions. The influence of the AC field parameters was studied by varying the field strength (10–250 V_{p-p} as a step function), time (1–60 min), and frequency (10^{-3} to 10^{5} Hz). The polymerization reaction was initiated using blue light with a hand-held light gun (Optilux 501) for 1 min while the field was being applied. The solidified samples were cured by blue light for another 10 min and then annealed at 110 °C in an oven overnight to further complete polymerization. The cured samples were first investigated with an optical microscope. For electrical and dielectric measurements, the samples were sectioned into rectangular blocks with a low-speed diamond saw, and then polished with a 1 μm diamond paste to expose fresh surfaces, which were electroded with a silver paste. For high-resolution scanning electron microscopy (HRSEM) studies, the samples were microtomed with a diamond knife. The AC conductivity and dielectric constants of the SWNT/UH composites were measured with a Novocontrol Broadband Dielectric Converter and a Solatron SI1260 Impedance/Gain-Phase Analyzer. Polarized Raman scattering spectra were collected using a Thermo Nicolet Almega™ dispersive visible Raman spectrometer. A 785 nm incident laser light excitation was used with a polarizer, and the laser beam was focused on the sample using an optical microscope. A low-excitation laser power (10 mW) was used to minimize sample heating. The actual dose of the laser drops lower than 10 μW after it passes through the spectrometer optics.

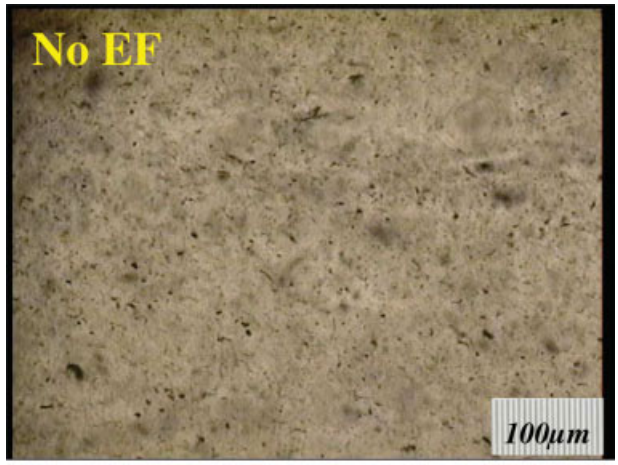

Figure 2. Optical micrographs of (a) SWNT/UH composite cured without electric field, (b) SWNT-UH composite cured with electric field (200 V_{p-p}, 10 Hz, 10 min). Note that the alignment of SWNTs along the applied electric field (EF↕). [Color figure can be viewed in the online issue, which is available at www.interscience.wiley.com.]

RESULTS AND DISCUSSION

Within the present experimental setup, there are three controllable parameters for influencing the degree of SWNT alignment: electric field strength, application time, and the frequency of the applied AC field. Optimal values for these parameters have been obtained by varying each in turn, while holding the other two constant. This actually requires an iterative process in which the values held fixed are determined by a number of preliminary experiments. In what follows, only the final set of experiments is described.

For the electric field strength optimization, the field application time was held fixed at 10 min while two AC frequencies were investigated, 100 Hz and 10 kHz. Various selected electric fields were applied as a step function at this condition. It was found that the degree of alignment was strongly dependent on the applied electric field and the same trends were observed with the two AC frequencies studied, 100 Hz and 10 kHz. No alignment was observed below 65 V_{p-p}, and alignment became noticeable at 75 V_{p-p} (37.5 V/2.3

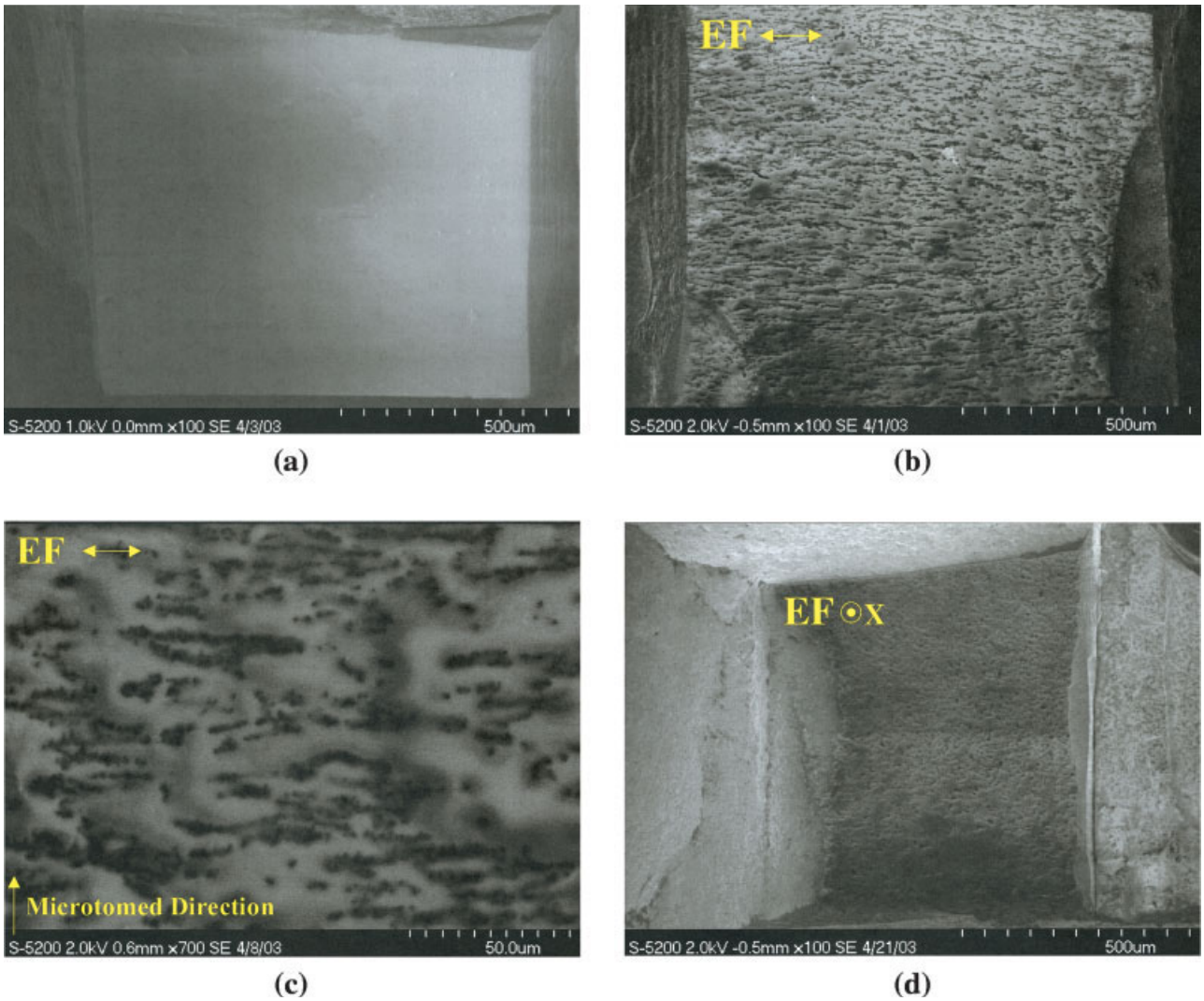

Figure 3. High-resolution scanning electron micrographs (HRSEM) of unaligned (a) and aligned SWNT/UH composites (200 V_{p-p}, 10 Hz, 10 min) microtomed surface parallel (b), (c) and perpendicular (d) to the electric field. Aligned nanotubes appeared as dark features. [Color figure can be viewed in the online issue, which is available at www.interscience.wiley.com.]

mm = 16.3 kV/m for a step function). The degree of alignment continued to increase up to a plateau value at 200 V_{p-p} (43.5 kV/m). Increasing the voltage beyond this point tended to induce more skewed alignment near the electrodes possibly due to excessive thermal energy. Beyond 300 V_{p-p}, the temperature of the composite increased significantly due to Joule heating (higher than 100 °C), which tended to locally disrupt or bend the aligned nanotubes. Next, the effect of field application time was studied at a fixed voltage of 200 V_{p-p} and frequency of 10 kHz. These experiments showed that alignment began almost immediately and grew with increasing field application time until saturation was observed at around 10 min. Finally, the effect of field frequency was studied at 200 V_{p-p} for an application time of 10 min. In this case, the degree of alignment grew with increasing frequency, saturating at 10 Hz. Interestingly the SWNTs were observed to align to some degree at frequencies as low as 0.001 Hz, which is effectively a DC condition, although this requires a much longer field application time.

Optical microscopy was used for initial, qualitative evaluation of the degree of alignment. Figure 2(a) shows an optical micrograph of a SWNT/UH composite cured without an electric field, which reveals a relatively uniform dispersion

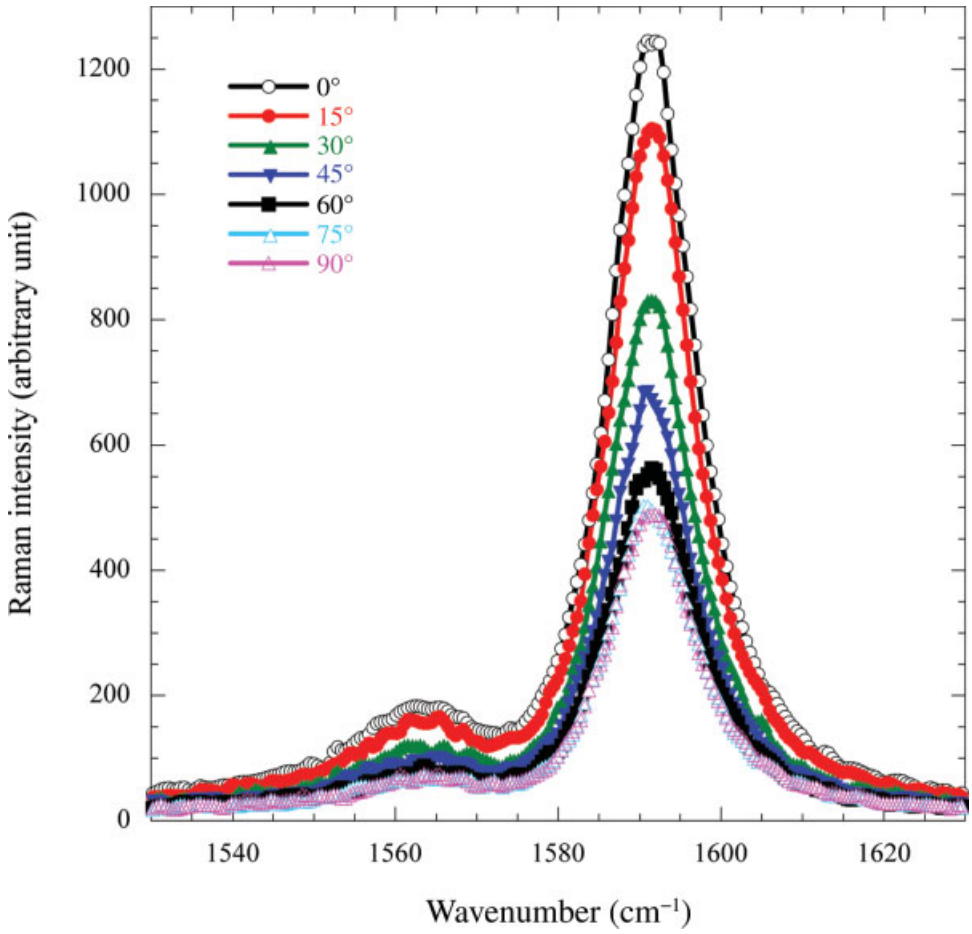

Figure 4. Polarized Raman spectra showing tangential peak of SWNTs aligned by AC electric field 200 V_{p-p}, 10 Hz, 10 min. [Color figure can be viewed in the online issue, which is available at www.interscience.wiley.com.]

overall with a few micrometer scale agglomerates and no preferential alignment or elongated features. Figure 2(b) shows a micrograph of the aligned composite prepared at 200 V_{p-p} and 10 Hz for 10 min, where aligned SWNT bundles are seen along the field direction and the micrometer scale agglomerates are also aligned with their elongated axes along the field direction.

More detailed microstructures of the aligned SWNTs were investigated with high-resolution scanning electron microscopy (HRSEM). The composites were microtomed either parallel or perpendicular to the field direction and examined without a conductive coating at a low voltage (below 1 kV). Figure 3(a) shows the microtomed surface of the unaligned sample, in which the nanotubes could not be imaged due to the nonconducting behavior of the sample. Figure 3(b) shows the SWNT aligned along the field, with some of the aligned clusters extending several hundred micrometers in length. The aligned clusters along the field are seen to be composed of a series of small SWNT clusters ranging from tens of nanometers to a few micrometers. Some of the aligned SWNT clusters lie parallel to one another and are connected with jagged or fray aligned clusters (coarsening). This aligned microstructure is reminiscent of the dielectrophoretic alignment and subsequent lateral coarsening of inclusions often observed in electrorheological or magnetorheological fluids.[23,26] This coarsening, which arises from the lateral migration among the aligned nanotubes, creates conductive percolation paths even at loadings as low as 0.03%. This permits formation of a stable electric field permitting visualization of the SWNTs that are part of the percolation paths. Although alignment of SWNT bundles and clusters was evident at higher magnification as shown in Figure 3(c), alignment of individual SWNTs in the clusters was not discernible due to

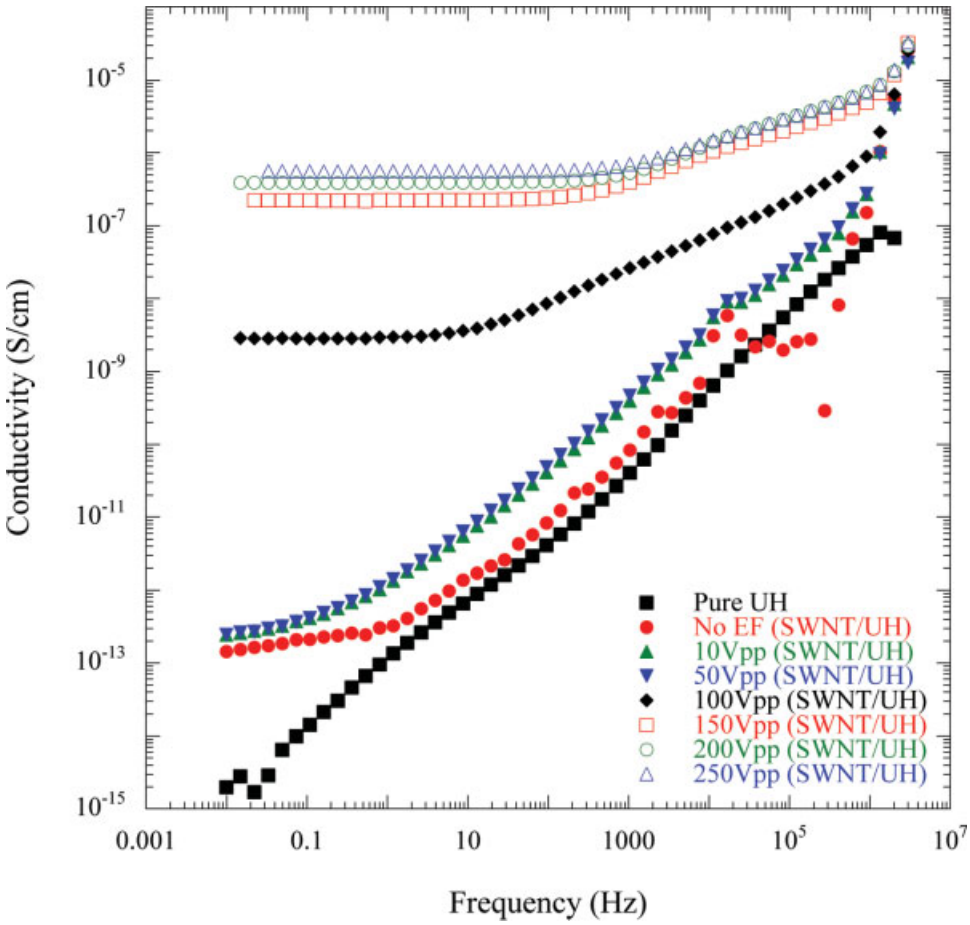

Figure 5. Conductivities of UH and SWNT/UH composites prepared at various electric fields (100 Hz, 10 min). [Color figure can be viewed in the online issue, which is available at www.interscience.wiley.com.]

the severe bleaching near the clusters. [Note that the small upward spikes shown in the aligned SWNTs in Fig. 3(c) result from microtoming.] It is also notable that there was little indication of any electrophoretic effect, which would be indicated by migration of SWNTs to the electrodes. Figure 3(d) shows a surface microtomed perpendicular to the electric field direction from the same aligned SWNT/UH composite. In this sample, evenly distributed, round SWNT clusters were observed, which are believed to be the cross sections of the aligned SWNT clusters shown in Figure 3(b). This indicates the distinct anisotropic nature of the aligned SWNT/UH composites and is similar to the anisotropic morphology observed in other composite systems containing spherical or equiaxed inclusions aligned under electric fields.[23]

The degree of alignment of SWNTs in the aligned composite was also assessed by polarized Raman spectroscopy. This characterization relies on the fact that the Raman intensity of the tangential mode of SWNTs is sensitive to the polarizer angle. The tangential mode intensity reaches a maximum when the polarized light is parallel to the nanotube axis[27] and decreases gradually as the angle of the polarizer increases from 0° (parallel to the nanotube axis) to 90° (perpendicular to the nanotube axis). The intensity begins to increase again as the angle of the polarizer increases from 90° to 180°. The tangential peaks (1591 cm^{-1}) of the polarized Raman spectra for the composite aligned at 10 Hz are shown for a series of angles in Figure 4. As expected, the maximum intensity was observed when the polarized light was parallel to the applied electric field direction (0°) and the smallest intensity appeared when the polarized light was perpendicular to the field direction (90°). Similar results were obtained for the composites aligned at frequencies ranging from 10 Hz to 100 kHz. The polarized Raman

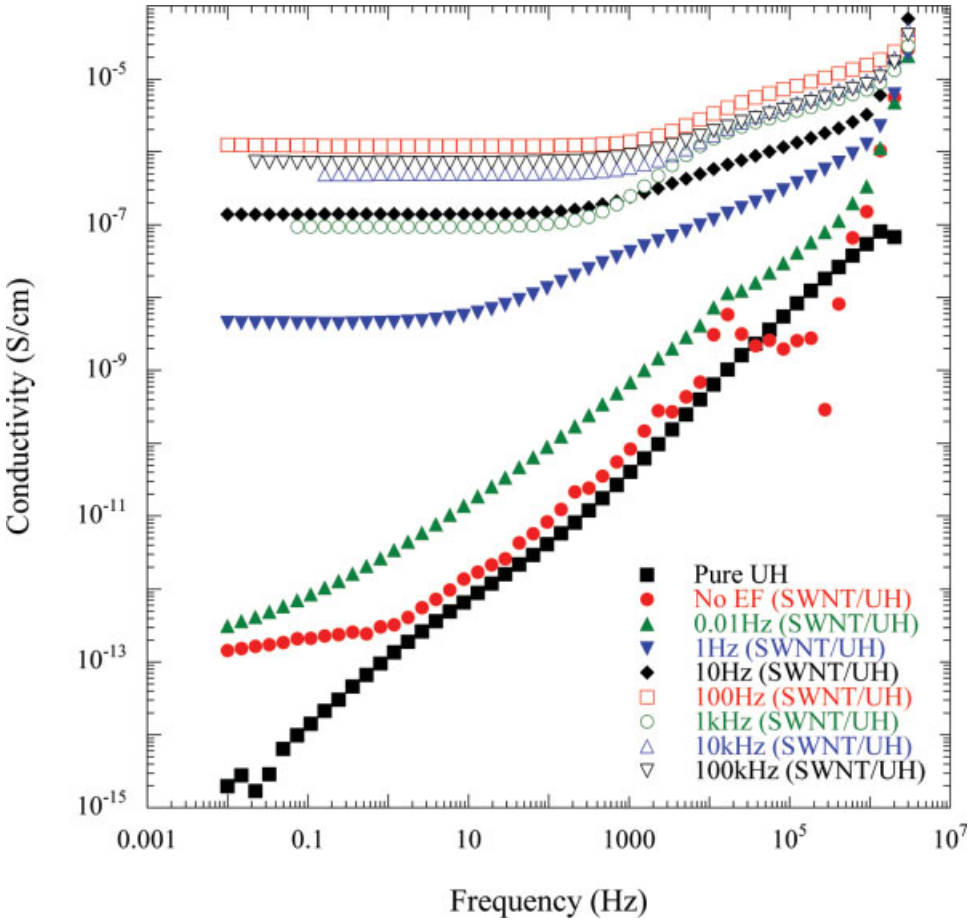

Figure 6. Conductivities of UH and SWNT/UH composites prepared at various frequencies (200 V_{p-p}, 10 min). [Color figure can be viewed in the online issue, which is available at www.interscience.wiley.com.]

results effectively demonstrate the preferential alignment of the individual SWNTs in the aligned SWNT bundles and clusters that resulted from the AC electric field.

Electrical Conductivity of SWNT/UH Composites

The conductivities of the pristine matrix resin UH and the unaligned and aligned composites containing 0.03 wt % SWNT are shown in Figure 5 as a function of the measurement frequency. Figure 5 shows the conductivities measured along the field direction for samples prepared at a series of applied voltages. At 1 Hz, the conductivities of the pristine resin and unaligned composite were 1.4×10^{-13} and 3.3×10^{-13} S/cm, respectively, revealing less than an order of magnitude increase in conductivity upon addition of 0.03 wt % SWNT. The conductivities of both of these samples increased linearly with the frequency on a logarithmic scale across most of the frequency range, indicating insulative behavior and therefore a lack of percolation at the 0.03 wt % SWNT loading. For the aligned composites, the conductivity of the samples in the aligned direction increases marginally up to 50 V_{p-p}, followed by a jump from 1.4×10^{-12} to 3.0×10^{-9} S/cm at 100 V_{p-p}. Further increases were observed for higher alignment fields up to saturation at around 150 V_{p-p}, where the conductivity is on the order of 10^{-7} S/cm. Metallic behavior was observed for the samples aligned above 100 V_{p-p}, as indicated by the relatively constant conductivity observed at low frequencies (below 10^2 Hz), which increases slightly at higher frequencies (above 10^2 Hz). These results indicate that the conductivity of the composites can be controlled over six orders of magnitude by controlling the strength of the aligning electric field.

The influence of the frequency of the applied electric field on the conductivity is shown in Figure 6. All of the aligned samples in the Figure 6 were formed under a field of 200 V_{p-p} for 10 min, at the various frequencies. The conductivity in the alignment direction of the composite prepared at 0.01 Hz, was slightly higher than that of the unaligned composite, but still showed insulating behavior. A significant increase was observed for the sample prepared at 1 Hz, with the conductivity increasing from 3.3×10^{-13} (no field) to 4.6×10^{-9} S/cm, which indicates a transition from insulating to metallic. At 10 Hz, the conductivity increases to 1.4×10^{-7} S/cm and reaches a plateau value of 10^{-6} S/cm at 100 Hz, saturating at higher frequencies. These results may indicate that, at very low frequencies, the misaligning forces, such as Brownian motion and electrophoretic force, are stronger than the aligning dielectrophoretic force, preventing or disrupting nanotube alignment. Above 1 Hz, where electrophoresis becomes insignificant, the aligning dielectrophoretic force becomes dominant, saturating above 100 Hz. Similarly to the previous case of field strength, these results show that the conductivity of SWNT/UH composites can be readily controlled by the AC frequency. Conductivities ranging from insulating (10^{-13} S/cm) to conductive (10^{-6} S/cm) can be achieved in the alignment direction with a 0.03 wt % SWNT loading, which is lower than the percolation concentration for an isotropic dispersion.[5,24,25] Although slight alignment was observed at lower frequencies (0.01 and 0.1 Hz), it was not reflected in the conductivity of the composite, suggesting that the aligned clusters of the SWNT bundles percolate above 0.1 Hz under these conditions.

In general, the concentration of conducting cylinders required to reach percolation is expected to increase with increasing degree of alignment, as shown in Figure 7. The observation of increasing conductivity with increasing alignment of SWNTs is unexpected based on the excluded volume percolation theory of cylindrical inclusions in an insulating matrix.[14,15] In the present composite, the AC field induces alignment of SWNTs, followed by attraction among the aligned SWNTs, which increases the effective aspect ratio of the SWNT inclusions. This increased effective aspect ratio decreases the percolation threshold. In addition, it is likely that the conductive path among the SWNTs bundles lies not only along the field direction, but also among the aligned clusters by lateral

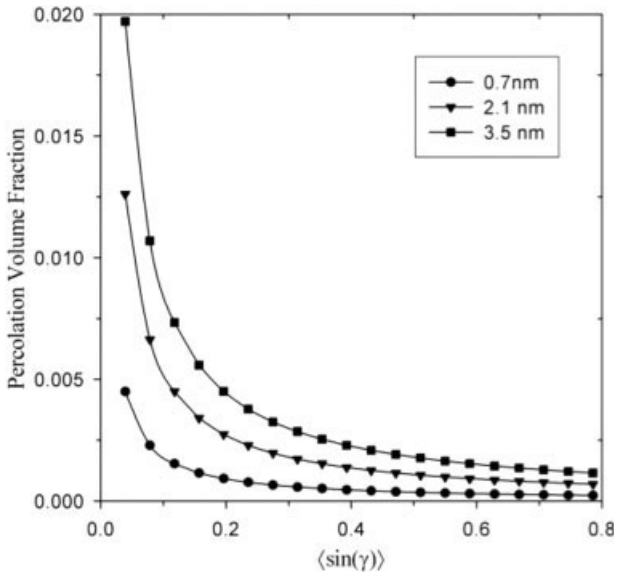

Figure 7. Percolation volume fraction as a function of orientation of SWNT with different nanotube diameters. ($<\sin(\gamma) \geq 0$ for perfect orientation, $= 1$ for random).

contacts. Remarkably, the conductivity of the composite perpendicular to the electric field alignment direction also increased with alignment by about two orders of magnitude, as shown in Figure 8. While the aligned clusters continued to grow by the accretion of small SWNT bundles or other aligned clusters longitudinally, the aligned clusters also attracted one another laterally. This lateral joining of aligned clusters resulted in the formation of crosslinks between aligned clusters with jagged or frayed ends, as shown in Figures 3(b,c) (coarsening). Figure 3(c) shows that some dots (cross sections of the aligned SWNTs) were connected with neighbors to form short chains. This early stage of coarsening is responsible for the relatively high conductivity of the composite in the direction perpendicular to the aligning field. This proposed sequence of formation of the aligned structure under an AC field was previously reported and described by a simple model.[23] In this picture, the electric field causes the SWNT bundles to first attract one another primarily along the field direction to form aligned SWNT bundle clusters, followed by lateral attractions that lead to crosslinking. Recall also the even distribution and nominally equivalent intercluster distances observed in Figure 3(d), which is consistent with previous observations.[23]

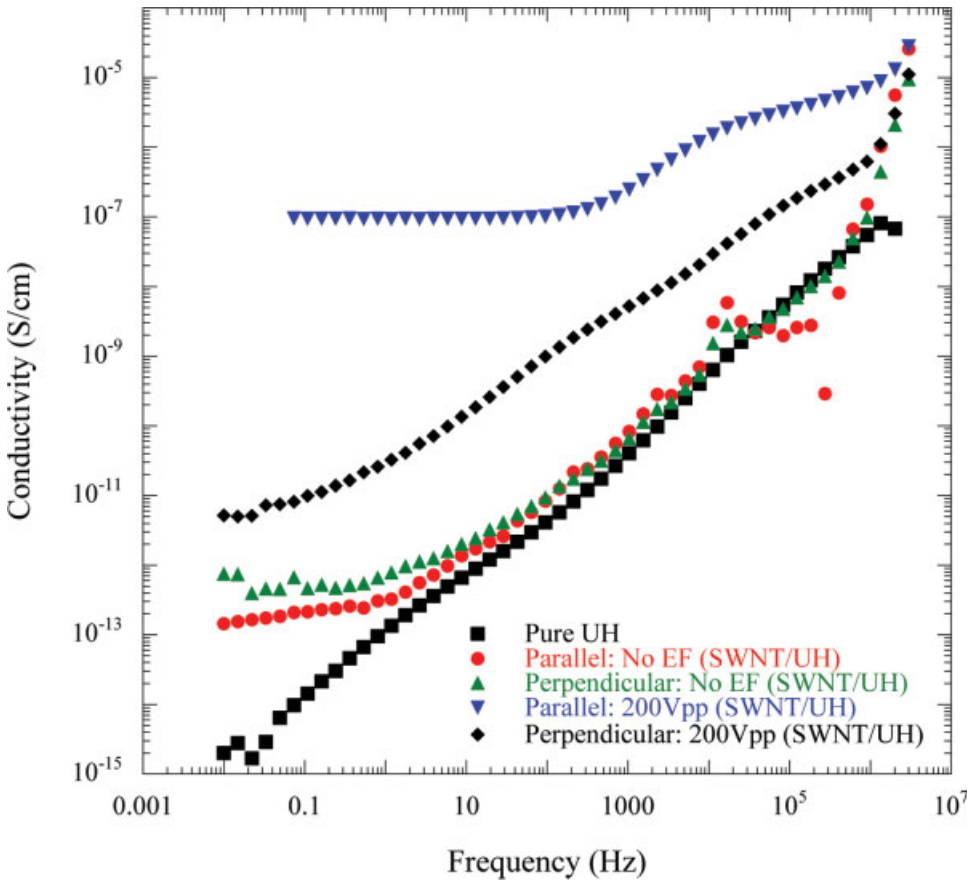

Figure 8. Conductivities of UH and SWNT/UH composites measured parallel and perpendicular to the field used in sample preparation. [Color figure can be viewed in the online issue, which is available at www.interscience.wiley.com.]

Dielectric Properties of SWNT/UH Composites

The dielectric constants of the pristine UH, unaligned, and aligned SWNT/UH composites (parallel to the alignment field) are shown as a function of frequency in Figure 9. All samples were aligned at 100 Hz for 10 min with the various applied field strengths. The dielectric constant of the pristine UH and the unaligned composite at 1 Hz were 5.2 and 25.2 at 0.03 wt %SWNT, respectively. For samples prepared under higher aligning fields, the dielectric constant increased in the same way as the conductivity. No significant increases were observed up to 50 V_{p-p}, followed by more significant increases up to 100 V_{p-p}, where the dielectric constant reaches values over 600 at 1 Hz. These increases continue up to a maximum value of around 1500 at 150 V_{p-p}, at which point saturation is observed. The composites prepared below 50 V_{p-p} exhibit an insulating material behavior, while those prepared above that show conductive behavior, which is consistent with the conductivity results.

The electric field frequency also strongly influenced the dielectric behavior of the composites, as shown in Figure 10. The composite aligned at 0.01 Hz exhibited little increase in dielectric constant over the unaligned composite, indicating lack of orientation at this frequency. For 1 Hz aligned samples, however, the dielectric constant increased up to 900 and exhibited strong dispersion at a measurement frequency of 100 Hz, suggesting the presence of a perocolative path of aligned nanotubes along the field direction. The dielectric constant saturated at a value of over 1000 for samples aligned at frequencies above 100 Hz. All of these results are completely consistent with the conductivity measurements. These experiments illustrate that the dielectric constant of the composites can be easily adjusted over three orders of magnitude by controlling the frequency and strength of the AC aligning field.

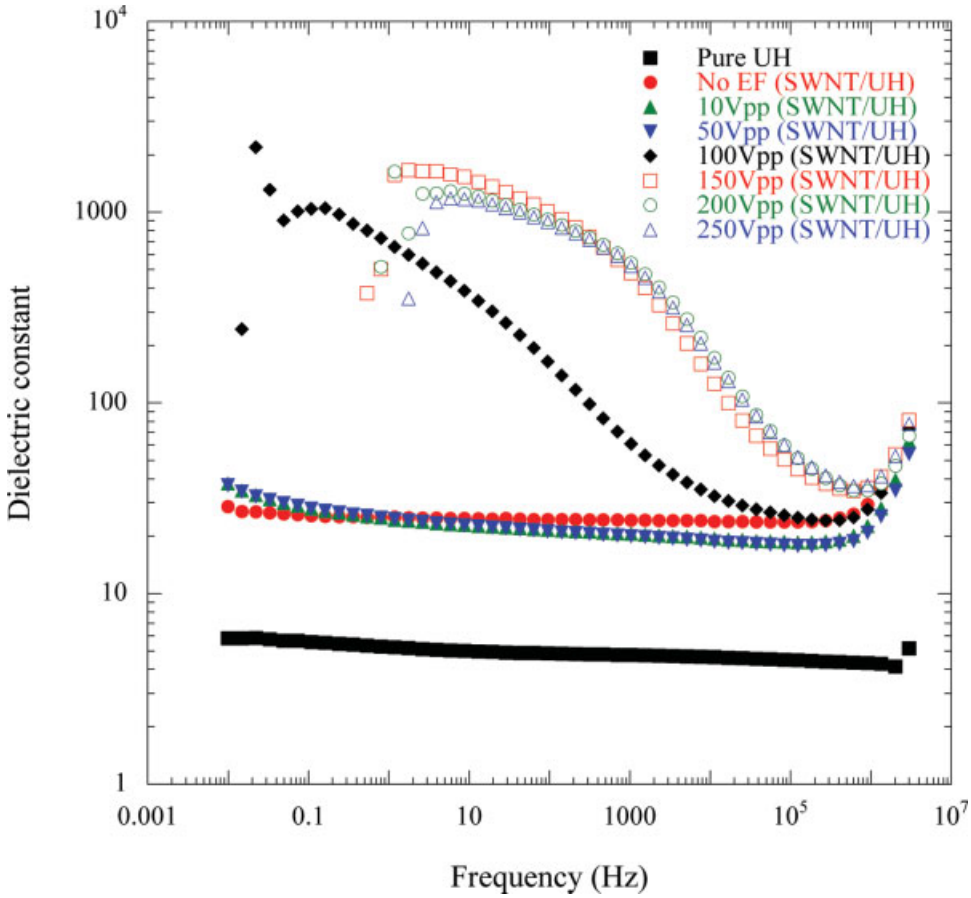

Figure 9. Dielectric constants of UH and SWNT/UH composites prepared at various electric fields. [Color figure can be viewed in the online issue, which is available at www.interscience.wiley.com.]

Having now established the alignment behavior of SWNTs in the UH matrix, it is of interest to attempt to understand these results within the context of a simple model, which may enable the design of improved systems. Alignment in this system arises from the field-induced polarization of the nanotubes and the attraction and repulsion between the induced dipole moments.[28] The dipolar interaction competes with the thermal randomization (*i.e.*, Brownian motion); therefore, alignment will generally only occur when the alignment force arising from dipolar interaction dominates.[28] For a spherical inclusion, the parameter defining the relative strengths of the dipolar interaction and thermal agitation is[29]

$$\lambda = \frac{\pi \varepsilon_0 \varepsilon_1 a^3 (\beta E)^2}{k_B T} \quad (1)$$

where ε_0 is the permittivity of free space (8.854×10^{-12} F/m), ε_1 is the relative dielectric constant of the liquid resin (about 4.9 at 20 Hz), a is the radius of the inclusion, E is the applied electric field, k_B is Boltzmann's constant (1.38×10^{-23}J K^{-1}), and T is the absolute temperature. When polarization arises from the mismatch of polarizability between the matrix and inclusion, β is given by $(\varepsilon_2 - \varepsilon_1)/(\varepsilon_2 + 2\varepsilon_1)$, where ε_2 is the relative dielectric constant of the inclusion. But when the conductivity of the inclusion or matrix dominates at low frequencies, β is given by $(\kappa_2 - \kappa_1)/(\kappa_2 + 2\kappa_1)$, where κ_1 and κ_2 are the conductivity of the matrix and inclusion, respectively. For the present system, since the inclusion is a cylindrical nanotube, the effective radius of the inclusion a may be replaced by the radius of gyration (R_g) of the nanotube. The length of the nanotube (L) was around 3 μm based on AFM study[30] and the radius of the nanotube (R) is about 0.5 nm. Assuming that the nano-

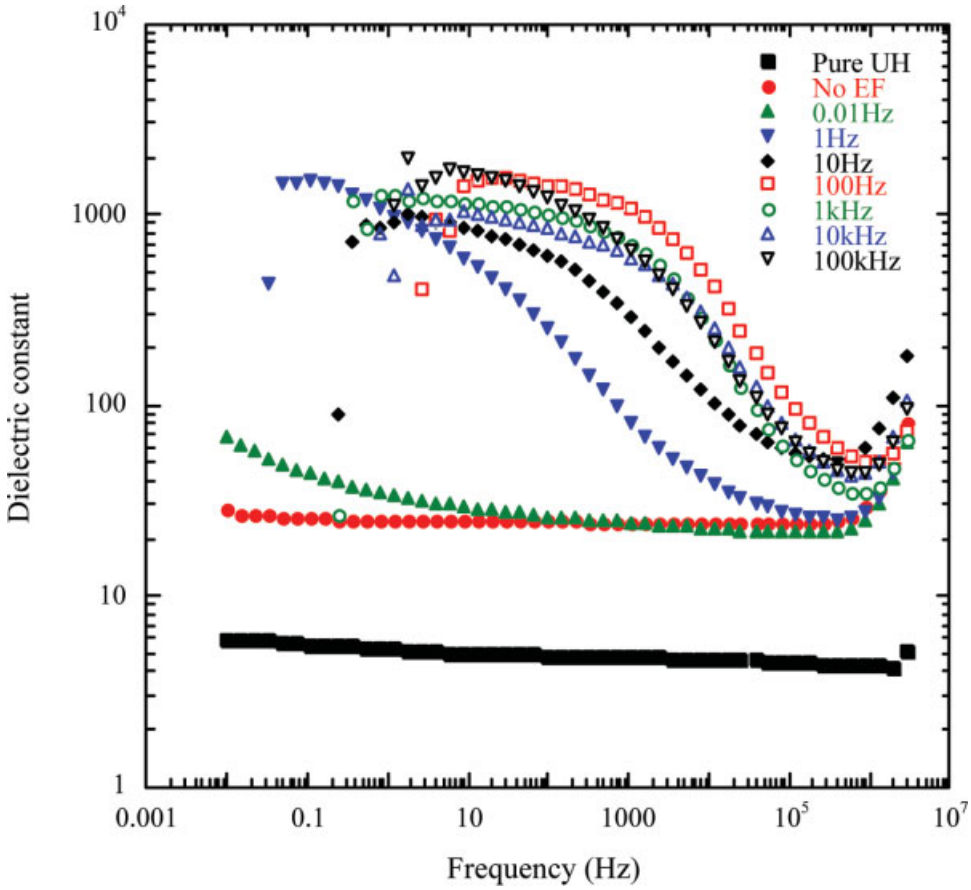

Figure 10. Dielectric spectra of pristine UH and SWNT/UH composites prepared at different frequencies. [Color figure can be viewed in the online issue, which is available at www.interscience.wiley.com.]

tube is a rigid cylinder, the radius of gyration of the nanotube is given by,[31]

$$a = R_g = ((R^2/2) + (L^2/12))^{1/2} \approx (L^2/12)^{1/2} \approx 0.87\,\mu\text{m}$$

The measured dielectric constant of a 2 wt % SWNT-polyimide composite was approximately 100,000 at 20 Hz.[13] Therefore, we can reasonably assume that the inclusion dipole coefficient *(β)* approaches 1. On the other hand, a DC conductivity of $\sim 10^2$ S/cm was obtained from fitting the conductivity of SWNT/polymer composties, using a two exponent phenomenological percolation equation.[26] This value, which is obtained from the conductivity of SWNT/polymer composites measured as a function of SWNT volume fraction, is comparable to those measured for SWNT mats (bucky papers).[32] The cured matrix is a capacitive insulating material with a conductivity of around 10^{-14} S/cm at 1 Hz, and while the liquid oligomer was more conductive, it still has a conductivity below 2×10^{-7} S/cm.[23] Using these values, β for DC or low frequency also approaches one. Therefore, in either case, the value β may be taken as one.

To achieve alignment, the parameter λ, which is the ratio of polarization energy to thermal energy, must be greater than one. For the present system, the critical effective nanotube size for alignment, assuming that polarization arises from the polarizibility of the fluid and nanotubes, can be calculated from eq 1 for the field strengths used for the alignment. The dielectric constant of the liquid is 4.9, and the temperature reached a maximum of 40 °C under the applied field (43.5 kV/m). If we assume that the dipole coefficient β is 1, the critical effective nanotube diameter is 0.67 μm at 43.5 kV/m (200 V_{p-p}) and 1.53 μm at 16.3 kV/m (75 V_{p-p}). Since the radius of gyration of nanotube was about 0.87 μm for 3 μm long nanotube, alignment is

likely to occur under the present field conditions. This conclusion is even more sound in light of the fact that the SWNT bundles are much longer than single tubes. This alignment can be accelerated with time once the aligned clusters grow, since the effective diameter of nanotubes continues to increase.

CONCLUSIONS

The results presented earlier show that the conductivity and dielectric properties of aligned SWNT/UH composites can be tuned over a broad range by proper control of the applied field strength, frequency, and time. The structure of the aligned composites was visually investigated using HRSEM, which showed clear distinctions from composites prepared by passive alignment using shear processing. The unusual crosslinked structure produced by the field alignment technique is expected to impart unique properties to the composite relative to those created by use of high shear (spinning, extrusion, and so on). These aligned SWNT polymer composites enable control over electrical and dielectric properties in addition to mechanical reinforcement, which will enable the development of multifunctional structural composites. The key feature of this approach is the novel ability to produce composites with the required properties for a specific application by simply tuning the applied field strength, frequency, and time.

C. Park and K. E. Wise appreciate the NASA University Research, Engineering and Technology Institute on Bio Inspired Materials (BIMat) under award no. NCC-1-02,037 for support in part.

REFERENCES AND NOTES

1. Saito, R.; Dresselhaus, G.; Dresselhaus, M. S. Physical Properties of Carbon Nanotubes; Imperial College Press: London, 1998.
2. Haggenmueller, R.; Gommans, H.; Rinzler, A.; Fischer, J.; Winey, K. Chem Phys Lett 2000, 330, 219.
3. Gong, X.; Liu, J.; Baskaran, S.; Voise, R. D.; Young, J. S. Chem Mater 2000, 12, 1049.
4. Qian, D.; Dickey, E.; Andrews, R.; Rantell, T. Appl Phys Lett 2000, 76, 2868.
5. Park, C.; Ounaies, Z.; Watson, K.; Crooks, R.; Connell, J.; Lowther, S. E.; Siochi, E. J.; Harrison, J. S.; St Clair, T. L. Chem Phys Lett 2002, 364, 303.
6. Kumar, S.; Dang, T. D.; Arnold, F. E.; Bhattacharyya, A. R.; Min, B. G.; Zhang, X.; Vaia, R. A.; Park, C.; Adams, W. W.; Hauge, R. H.; Smalley, R. E.; Ramesh, S.; Willis, P. A. Macromolecues 2002, 35, 9039.
7. Siochi, E. J.; Working, D. C.; Park, C.; Lillehei, P. T.; Rouse, J.; Topping, C. C.; Bhattacharyya, A. R.; Kumar, S. Compos B 2004, 35, 439.
8. Baughman, R. H.; Cui, C.; Zakhidov, A. A.; Iqbal, Z.; Barisci, J. N.; Spinks, G. M.; Wallace, G. G.; Mazzoldi, A.; De Rossi, D.; Rinzler, A. G.; Jaschinski, O.; Roth, S.; Kertesz, M. Science 1999, 284, 1340.
9. Wood, J. R.; Wagner, H. D. Appl Phys Lett 2000, 76, 2883.
10. Kim, P.; Lieber, C. M. Science 1999, 286, 2148.
11. Kong, J.; Franklin, N. R.; Zhou, C.; Chapline, M. G.; Peng, S.; Cho, K.; Dai, H. Science 2000, 287, 622.
12. Sumanasekera, G.; Adu, C.; Fang, S.; Eklund, P. Phys Rev Lett 2000, 85, 1096.
13. Ounaies, Z.; Barnes, C.; Park, C.; Harrison, J. S.; Lillehei, P. T. (Submitted for publication).
14. Balberg, I.; Binenbaum, N.; Wagner, N. Phys Rev Lett 1984, 52, 1465.
15. Balberg, I.; Binenbaum, N.; Alexander, S.; Wagner, N. Phys Rev B 1984, 30, 3933.
16. Yamamoto, K.; Akita, S.; Nakayama, Y. Jpn J Appl Phys 1996, 35, L917.
17. Yamamoto, K.; Akita, S.; Nakayama, Y. J Phys D: Appl Phys 1998, 31, L34.
18. Chen, X. Q.; Saito, T.; Yamada, H.; Matsushige, K. Appl Phys Lett 2001, 78, 3714.
19. Nagahara, L. A.; Amlani, I.; Lewenstein, J.; Tsui, R. K. Appl Phys Lett 2002, 80, 3826.
20. Krupke, R.; Hennrich, F.; Löhneysen, H. V.; Kappes, M. M. Science 2003, 301, 344.
21. Kimural, T.; Ago, H.; Tobita, M.; Ohshima, S.; Kyotani, M.; Yumura, M. Adv Mater 2002, 14, 1380.
22. Martina, C. A.; Sandler, J. K. W.; Windle, A. H.; Schwarz, M.-K.; Bauhofer, W.; Schulte, K.; Shaffer, M. S. P. Polymer 2005, 46, 877.
23. Park, C.; Roberston, R. E. Mater Sci Eng A 1998, 257, 295.
24. McLachlan, D. S.; Chiteme, C.; Park, C.; Wise, K. E.; Lowther, S. E.; Lillehei, P. T.; Siochi, E. J.; Harrison, J. S. J Polym Sci Part B: Poly Phys 2005, 43, 3273.
25. Ounaies, Z.; Park, C.; Wise, K. E.; Siochi, E. J.; Harrison, J. S. Comp Sci Technol 2003, 63, 1637.
26. Tang, X.; Zhang, X.; Tao, R.; Rong, Y. J Appl Phys 2000, 87, 2634.
27. Rao, A. M.; Jorio, A.; Pimenta, M. A.; Dantas, M. S. S.; Saito, R.; Dresselhaus, G.; Dresselhaus, M. S. Phys Rev Lett 2000, 84, 1820.
28. Pohl, H. A. Dielectrophoresis: The Behavior of Neutral Matter in Nonuniform Electric Fields; Cambridge University Press: Cambridge, 1978.
29. Gast, A. P.; Zukoski, C. F. Adv Colloid Interface Sci 1989, 30, 153.
30. Park, C.; Crooks, R. E.; Siochi, J.; Harrison, J. S.; Kenik, E.; Evans, N. Nanotechnology 2003, 14, L11.
31. Rubinstein, M.; Colby, R. H. Polymer Physics; Oxford University Press: New York, 2003; p 64.
32. Sreekumar, T. V.; Liu, T.; Kumar, S.; Ericson, L. M.; Hauge, R. H.; Smalley, R. E. Chem Mater 2003, 15, 175.